Electron leak from NDUFA13 within mitochondrial complex I attenuates ischemia-reperfusion injury via dimerized STAT3

Hengxun Hu[a,1], Jinliang Nan[a,1], Yong Sun[a,1], Dan Zhu[a], Changchen Xiao[a], Yaping Wang[a], Lianlian Zhu[a,b], Yue Wu[a,b], Jing Zhao[a,b], Rongrong Wu[a], Jinghai Chen[a,c], Hong Yu[a], Xinyang Hu[a], Wei Zhu[a,2], and Jian'an Wang[a,2]

[a]Cardiovascular Key Laboratory of Zhejiang Province, Department of Cardiology, The Second Affiliated Hospital, Zhejiang University School of Medicine, Hangzhou 310009, Zhejiang Province, China; [b]Clinical Research Center, The Second Affiliated Hospital, Zhejiang University School of Medicine, Hangzhou 310009, China; and [c]Institute of Translational Medicine, Zhejiang University, Hangzhou 310029, China

Edited by J. G. Seidman, Harvard Medical School, Boston, MA, and approved September 1, 2017 (received for review March 23, 2017)

The causative relationship between specific mitochondrial molecular structure and reactive oxygen species (ROS) generation has attracted much attention. NDUFA13 is a newly identified accessory subunit of mitochondria complex I with a unique molecular structure and a location that is very close to the subunits of complex I of low electrochemical potentials. It has been reported that down-regulated NDUFA13 rendered tumor cells more resistant to apoptosis. Thus, this molecule might provide an ideal opportunity for us to investigate the profile of ROS generation and its role in cell protection against apoptosis. In the present study, we generated cardiac-specific tamoxifen-inducible NDUFA13 knockout mice and demonstrated that cardiac-specific heterozygous knockout (cHet) mice exhibited normal cardiac morphology and function in the basal state but were more resistant to apoptosis when exposed to ischemia-reperfusion (I/R) injury. cHet mice showed a preserved capacity of oxygen consumption rate by complex I and II, which can match the oxygen consumption driven by electron donors of *N,N,N′,N′*-tetramethyl-p-phenylenediamine (TMPD)+ascorbate. Interestingly, at basal state, cHet mice exhibited a higher H_2O_2 level in the cytosol, but not in the mitochondria. Importantly, increased H_2O_2 served as a second messenger and led to the STAT3 dimerization and, hence, activation of antiapoptotic signaling, which eventually significantly suppressed the superoxide burst and decreased the infarct size during the I/R process in cHet mice.

mitochondria | NDUFA13 | STAT3 | reactive oxygen species | hydroxyl peroxide

Mitochondria are the powerhouses of living cells, with generating ATP through oxidative phosphorylation as their main duty (1). However, mitochondria can become the major sites of reactive oxygen species (ROS) generation in the pathological process, causing significant cell damage, for example, in the process of ischemia-reperfusion (I/R) injury (2). Studies have shown that both complex I (3) and complex III (4) are the two important sites for ROS generation. There is mounting evidence that complex I might be the main source of ROS generation in intact mammalian mitochondria in vitro (5, 6). As the first segment of the electron transfer chain, complex I can be functionally dissected into several components, including a flavin mononucleotide (FMN) moiety, iron-sulfur clusters, and a ubiquinone-binding domain (7); each segment has a special structure and unique electrochemical potentials (7). Of note, the unique electrochemical potential pertaining to these components can determine the specific species of ROS generated through the related components of complex I (8). However, ROS are also important signaling molecules. Moderate levels of ROS have been reported to promote cell proliferation and survival (9, 10). Interestingly, inhibition of complex I activity could offer significant protection against I/R injury (2, 11), which can be attributed to decreased ROS generation during the reperfusion period (11). Given that knockdown of any component of the core subunit, such as NDUFS and NDUFV within complex I, in genetic mouse models can be lethal (7), it is tempting to determine to what extent a decrease in complex I activity can offer protection against stress by generating an appropriate amount of ROS without compromising energy transduction and the generation of ATP.

Studies have shown decreased expression of NDUFA13, a supernumerary subunit of complex I, in various tumors (12). As an accessory subunit of complex I, NDUFA13 (GRIM-19) is, to the best of our knowledge, the only protein that contains a transmembrane helix (TMH) structure that can penetrate both Iα and Iλ, two important structures situated within complex I (13). Importantly, down-regulation of NDUFA13 expression can render the tumor cells more resistant to chemotherapy (14). In addition, monoallelic loss of NDUFA13 promotes tumorigenesis in mice, which is associated with decreased apoptosis (14). In contrast, administration of IFN/retinol can induce NDUFA13 expression in MCF-7 cells, which resulted in a 50% increase in apoptotic cells (15), indicating its proapoptotic effects (14). Despite an association between NDUFA13 expression and apoptosis level, it remains unknown whether ROS generation is involved in changes in tumor apoptosis activity when NDUFA13 is expressed at low levels. Of note, the location of NDUFA13 within complex I is very close to segments with lower electromechanical potentials (7); this special location might offer

Significance

Reactive oxygen species (ROS) generation due to electron leak from the mitochondria may be involved in physiological or pathological processes. NDUFA13 is an accessory subunit of mitochondria complex I with a unique molecular structure and is located close to FeS clusters with low electrochemical potentials. Here, we generated cardiac-specific conditional NDUFA13 heterozygous knockout mice. At the basal state, a moderate down-regulation of NDUFA13 created a leak within complex I, resulting in a mild increase in cytoplasm localized H_2O_2, but not superoxide. The resultant ROS served as a second messenger and was responsible for the STAT3 dimerization and, hence, the activation of antiapoptotic signaling, which eventually significantly suppressed the superoxide burst and decreased the infarct size during the ischemia-reperfusion process.

Author contributions: H.H., J.N., Y.S., D.Z., Y. Wang, Y. Wu, R.W., J.C., H.Y., X.H., W.Z., and J.W. designed research; H.H., D.Z., C.X., L.Z., Y. Wu, and J.Z. performed research; J.N., Y.S., C.X., Y. Wang, L.Z., R.W., X.H., and W.Z. contributed new reagents/analytic tools; H.H., J.N., Y. Wang, L.Z., Y. Wu, J.Z., J.C., H.Y., X.H., and W.Z. analyzed data; and H.H., Y.S., D.Z., W.Z., and J.W. wrote the paper.

The authors declare no conflict of interest.

This article is a PNAS Direct Submission.

Freely available online through the PNAS open access option.

[1]H.H., J.N., and Y.S. contributed equally to this work.

[2]To whom correspondence may be addressed. Email: wangjianan111@zju.edu.cn or weizhu65@zju.edu.cn.

This article contains supporting information online at www.pnas.org/lookup/suppl/doi:10.1073/pnas.1704723114/-/DCSupplemental.

an opportunity to establish a unique profile of ROS generation within the mitochondria when NDUFA13 is down-regulated. It has also been reported that decreased NDUFA13 expression is associated with enhanced STAT3 signaling, which may also account for the augmented survival in tumor cells (14, 16–18). Again, it remains largely unknown whether and how STAT3 activation is related to ROS generation induced by down-regulated NDUFA13.

In the present study, we generated cardiac-specific NDUFA13 knockout mice, which would allow us to investigate the profile of ROS generation when NDUFA13 was moderately down-regulated and how resultant ROS offer the protection for cells, specifically for the myocardium against I/R injury. Further, we aimed to elucidate whether and how the activated STAT3 signaling was also responsible for the protection of the heart.

Results

Moderate NDUFA13 Down-Regulation Confers Protection Against Hypoxia/Reoxygenation-Induced Cell Injury. To test the roles of NDUFA13 in cardiomyocytes, we transfected H9C2 cells with NDUFA13-targeting siRNA and showed that a 100 μmol/L concentration of siRNA-NDUFA13 resulted in a 30% decrease and a 200 μmol/L siRNA-NDUFA13 resulted in a 60% decrease in NDUFA13 expression (Fig. 1*A*). Note that mitochondrial membrane potential (MMP) was impaired at the high (200 μmol/L) dose of siRNA-NDUFA13, but not at the low dose (100 μmol/L) (Fig. S1*A*). Interestingly, the resultant-moderate decrease in NDUFA13 expression was associated with a decrease in TUNEL-positive cells when these cells were exposed to hypoxia for 6 h followed by reoxygenation for 18 h (Fig. 1*B*). However, a severe decrease in NDUFA13 expression failed to elicit any protection against hypoxia/reoxygenation (H/R)-induced apoptosis (Fig. 1*B*). Consistent with TUNEL staining, the same pattern of changes was observed in cleaved caspase-3 and caspase-9 expression, with the protective effects being present only when NDUFA13 was moderately down-regulated (Fig. 1*A*). However, cleaved caspase-8, which is involved in the extrinsic apoptotic pathway, did not show significant changes (Fig. 1*A*). Meanwhile, phosphorylation level of apoptosis signal-regulating kinase at threonine 845 (pASK1^{Thr845}) and its downstream target p-JNK level were not affected (Fig. S1*B*). In summary, the data suggested that a moderate decrease in NDUFA13 expression conferred a significant protection against apoptosis obtained from H9C2 cells.

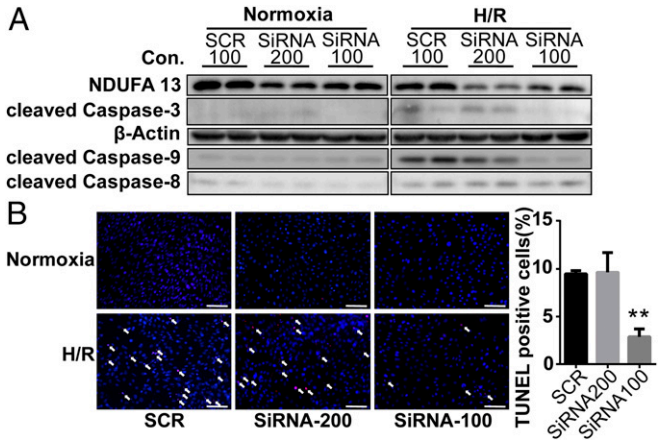

Fig. 1. (*A*) H9C2 cells tr insulintransferrin-selenium ansfected with different concentrations of siRNA targeting rat NDUFA13 were exposed to normoxia or H/R. NDUFA13 and cleaved caspase-3, caspase-9, and caspase-8 expression levels were detected by Western blot, with β-actin as the loading control (n = 4 per group). (*B*) The percentage of TUNEL-positive cells (marked by white arrow) quantified and shown in the bar graph, $^{**}P < 0.01$ vs. scramble (SCR) transfection (n = 3 per group). (Scale bars: 100 μm.)

Characterization of Tamoxifen-Inducible Cardiac-Specific NDUFA13 Transgenic Mice. To further investigate how a slight decrease in NDUFA13 offers cardiac protection against apoptosis in vivo, we generated a cardiac-specific conditional NDUFA13 knockout mouse model (see details in *Methods*). Eight-week-old Myh6Cre^{+}NDUFA13$^{flox/flox}$ (cHomo) mice and age-matched Myh6Cre^{+}NDUFA13$^{flox/-}$ (cHet) mice were studied, and Myh6Cre^{-}NDUFA13$^{flox/-}$ mice were used as controls (CON). i.p. injections of tamoxifen (see *Methods* for detailed information) were administered to each mouse. To evaluate the time course of changes in NDUFA13 expression after tamoxifen treatment, on days 1, 4, 7, 10, 13, and 16 after tamoxifen administration, three mice from each group were killed, respectively, and the hearts were obtained to test the relationship between NDUFA13 expression and the ATP level. Tamoxifen time-dependently down-regulated NDUFA13 expression in both cHomo and cHet mice. A moderate decrease in NDUFA13 expression was observed on day 16 in cHet mice, whereas a moderate decrease was detected as early as day 1 in cHomo mice, and an almost 80% decrease was observed on day 16 after tamoxifen treatment (Fig. 2*A*). Interestingly, cHet mice did not exhibit any changes in ATP level in the heart compared with CON mice (Fig. 2*B*), whereas cHomo exhibited a significant time-dependent decrease in ATP content in the heart, with a significant change detected as early as 4 d after tamoxifen administration (Fig. 2*B*). Being consistent with quantification of ATP levels in the heart tissue, cHomo mice experienced sudden death, whereas cHet and CON mice shared a similar survival rate as demonstrated by Kaplan–Meyer's survival curves (Fig. 2*C*). Based on these data, we used only cHet mice to test whether a moderate NDUFA13 down-regulation had cardioprotective effects against I/R-induced stress. To further confirm that cHet mice did not exhibit any abnormalities in cardiac structure and function, echocardiographic examinations were performed on nine cHet and nine CON mice on day 28 after tamoxifen administration, and the results demonstrated that normal cardiac structure and function were observed in the cHet mice compared with the CON mice (Fig. 2*D*, Fig. S2*A*, and Table S1). The mice were then killed for further analysis. Compared with CON mice, cHet mice did not exhibit any significant changes in cardiac ultrastructure as demonstrated by transmission electronic microscopy (TEM) examination (Fig. 2*E*), and mitochondrial morphology (Fig. 2*E*) was similar between cHet and CON mice. Protein expression of several key mitochondrial components, including ATP2A2, NDUFB8, and SDHC (for ATP generation); ATP5A (for ATP consumption); and PGC-1α (a key transcription factor that orchestrates mitochondrial biogenesis) were not altered (Fig. 2*F* and Fig. S2*B*). NDUFA13 expression in other tissues, such as the brain, lung, and liver, was similar between cHet and CON mice (Fig. 2*F* and Fig. S2*B*), further confirming a reliable cardiac-specific NDUFA13 knock-down mouse model. Using freshly isolated mitochondria from the hearts, substrate-driven mitochondrial respiratory function was analyzed. With the presence of ADP, substrate-driven oxygen consumption rate (OCR) was measured for complex I (addition of pyruvate and malate followed by rotenone, an inhibitor of complex I), complex II (succinate), and complex IV [*N*,*N*,*N*′,*N*′-tetramethyl-p-phenylenediamine (TMPD)/ascorbate followed by azide, an inhibitor of complex IV]. The data showed a decrease in substrate-driven OCR of complex I in cHet mice; however, OCR by combination of complex I and II could, in compensation, match OCR driven by the electron donor (TMPD/ascorbate) through complex IV (Fig. 2*G* and Fig. S2*C*). In summary, we generated a conditional cardiac-specific NDUFA13 knockout mouse model; cHet mice exhibit normal cardiac structure and function at baseline, which was associated with a compensatory normal mitochondrial function and ATP production.

NDUFA13 Down-Regulation Protected Mouse Hearts from I/R Injury. To test whether a moderate down-regulation of NDUFA13 could protect the heart from I/R injury, we generated an in vivo cardiac I/R injury model in both cHet and CON mice, by coronary artery ligation for 45 min followed by 3 h of reperfusion. Interestingly, we observed a significant decrease in the infarct size (IS) in cHet mice

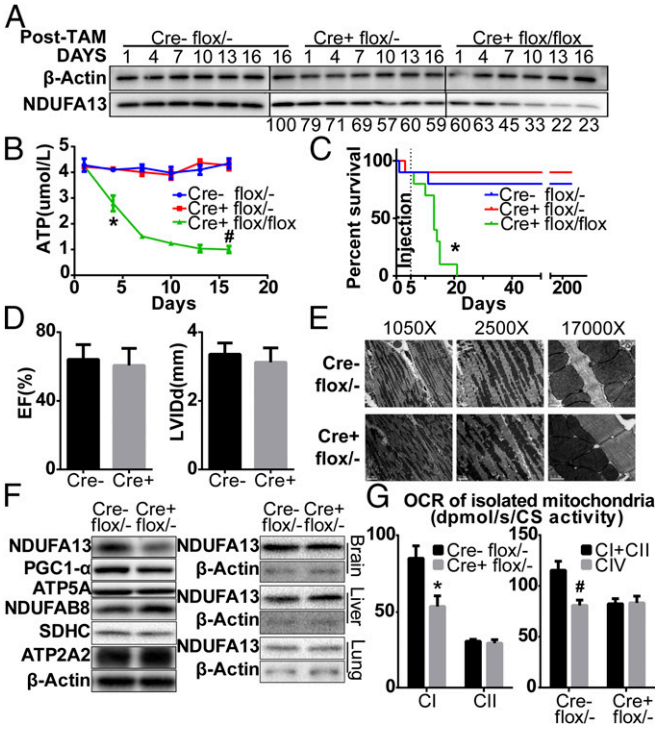

Fig. 2. Three groups of mice, including cHet (Cre+flox/-), cHomo (Cre+flox/flox), and CON (Cre-flox/-), were studied. (*A*) The time course of changes in NDUFA13 expression in the heart were evaluated at the indicated time points by Western blot (representative bands shown with its expression level relative to that in Cre-flox/- mice. β-Actin as a loading control, $n = 3$ mice per group). (*B*) ATP levels (micromoles per liter) quantified at the indicated time points (*$P < 0.05$; #$P < 0.05$ vs. Cre-flox/- group, respectively); (*C*) Kaplan–Meier survival curves were generated for the three groups of mice over a prospective observation period of 240 d ($n = 10$ mice per group. *$P < 0.05$ vs. Cre-flox6/- group). "Injection" indicates the date of the completion of tamoxifen administration. (*D*) Echocardiography performed for both cHet and CON mice on day 28 after tamoxifen administration; ejection fraction (EF) and LVIDd quantified in the bar graphs ($n = 9$ mice per group). (*E*) TEM performed on samples from Cre+flox/- and Cre-flox/- mice on day 28 after tamoxifen administration. (Scale bars: *Left*, 5 μm; *Center*, 2 μm; *Right*, 0.5 μm.) (*F*) Different components of the mitochondrial respiratory complexes were quantified by Western blot in both group mice with representative bands shown ($n = 3$ per group). NDUFA13 expression levels were quantified in other tissue with β-actin as a loading control ($n = 3$ mice per group). (*G*) OCR was measured by O2k-Fluorometry (*$P < 0.05$ vs. Cre-flox/- mice; #$P < 0.05$, comparison within Cre-flox/- group mice).

compared with CON mice (Fig. 3*A*). Quantification of apoptotic level at the peri-infarct area showed that TUNEL-positive cardiomyocytes were significantly decreased in cHet mice that underwent I/R intervention compared with CON mice that experienced the same I/R insult (Fig. 3*B*). The decrease in apoptosis was also confirmed when peri-infarct heart tissue was used for Western blot analysis, showing a significant decrease in cleaved caspase-3 expression in cHet mice compared with CON mice (Fig. 3*C*). The same pattern of changes was also seen in cytochrome C (cytoC) release into the cytosol, showing much less leak in cHet mice following an I/R injury compared with CON mice that were exposed to I/R injury (Fig. 3*D*). Taken together, these results strongly supported that moderate NDUFA13 down-regulation confers protection against I/R injury through the suppression of apoptosis.

Down-Regulated NDUFA13 Expression Is Associated with Increased Basal ROS Generation. To investigated the profile of ROS generation by a partial loss of NDUFA13, we freshly isolated mitochondria from both cHet and CON mice that were treated with tamoxifen. We measured OCR and H_2O_2 levels simultaneously with the Oroboros O2k system. Using different substrates and blockers specific for complex I and complex III, we demonstrated that succinate caused a significant amount of H_2O_2 through reverse electron transport (RET) in the mitochondria from CON mice, this RET-induced ROS generation can be blocked by rotenone. In contrast, mitochondria from cHet mice exhibited a much smaller RET-induced H_2O_2, indicating an interrupted RET process. Importantly, however, further addition of pyruvate and malate resulted in an unexpected increase in H_2O_2 level in cHet mice, which was not observed in CON mice. A final addition of antimycin A resulted in a similar degree of increment in H_2O_2 in both CON and cHet mice (Fig. 4*A* and Fig. S3*A*).

To confirm cHet mice mainly generated H_2O_2, we used mitoSOX red to detect the superoxide levels within the mitochondria. We cross-bred cHomo ($NDUFA13^{flox/flox}$) mice with wild-type littermates ($NDUFA13^{WT}$) to generate NDUFA13 heterozygous ($NDUFA13^{flox/-}$) mice. The neonatal cardiomyocytes (NMCMs) were then obtained from these mice and transfected with adenovirus-containing Cre recombinase (Ad-Cre) or an empty vector as a normal control (Ad-NC). The effect of Cre recombinase on NDUFA13 expression in NMCMs was confirmed (Fig. S3*B*). Using mitoSOX Red as a probe, we showed that at basal state, NMCMs treated with Ad-Cre or Ad-NC had a similar level of superoxide (Fig. 4*B*), importantly, Ad-Cre–treated NMCMs exhibited much lower superoxide levels compared with Ad-NC–treated NMCMs when exposed to H/R (Fig. 4*B*).

NMCMs obtained from $NDUFA13^{flox/-}$ mice that had been treated with Ad-Cre or Ad-NC as described above were infected adenovirus containing mitochondrial targeting HyPer (mito-Hyper) or cytoplasm-targeting HyPer (cyto-HyPer) for measuring H_2O_2 in the mitochondria and in the cytoplasm, respectively (Fig. S3*C*). At basal state, H_2O_2 level detected by cyto-HyPer was higher in Ad-Cre–treated NMCMs than that in Ad-NC–treated cells; however, the differences between the two cell groups were absent when measuring H_2O_2 levels in the mitochondria, further confirming that a leak was present within complex I when NDUFA13 was down-regulated. Interestingly, following H/R, a burst of H_2O_2 was present in both cytosol and mitochondria of Ad-NC–treated NMCMs, which was much less in the mitochondria in Ad-Cre–treated cells (Fig. 4*C*).

The Molecular Structure of NDUFA13 in Maintaining the Integrity of Mitochondrial Membrane. We then designed several adenoviruses that contained different truncated NDUFA13 mutants, including Ad-1 (with a deletion of amino acid 40–50), Ad-2 (a deletion of amino acids 70–80), Ad-3 (a deletion of amino acids 110–120), Ad-NDUFA13 (a wild-type full-length NDUFA13 as a normal control), and Ad-Vector (an empty vector as a negative control) (Fig. S4*A*). By transfecting these various vectors respectively back into NDUFA13-depleted NMCMs (isolated from $NDUFA13^{flox/flox}$ mice and pretreated with Ad-Cre with the efficiency confirmed in Fig. S4*B*), we can measure both MMP and H_2O_2 generation to test the role of the TMH in NDUFA13. The NMCMs transfected with Ad-Cre exhibited a significant decrease in MMP compared with NMCMs transfected with Ad-NC, as shown by measuring the fluorescence intensity (Fig. S4*C*) or by flow cytometry (Fig. S4*D*) following TMRM staining. Ad-NDUFA13, Ad-1, Ad-2, Ad-3, or Ad-Vector was then transfected into endogenous NDUFA13-depleted NMCMs (with the efficiency of transfection confirmed in Fig. S4*E*). Ad-1 failed to colocalize with the mitochondria (Fig. S4*F*) to maintain the MMP (Fig. S4*G*), whereas Ad-2 and Ad-3 could fully mimic and compensate for wild-type NDUFA13 (Fig. S4 *F* and *G*). Importantly, the same pattern of changes was seen when cyto-Hyper was cotransfected into NDUFA13-depleted NMCMs to test if increased cytosolic H_2O_2 level in Ad-Cre–treated NMCMs was abolished by putting back different truncated NDUFA13 mutants (Fig. S4*H*). These results strongly supported an essential role for TMH domain in maintaining the MMP, which also might serve as a main source of H_2O_2 generation.

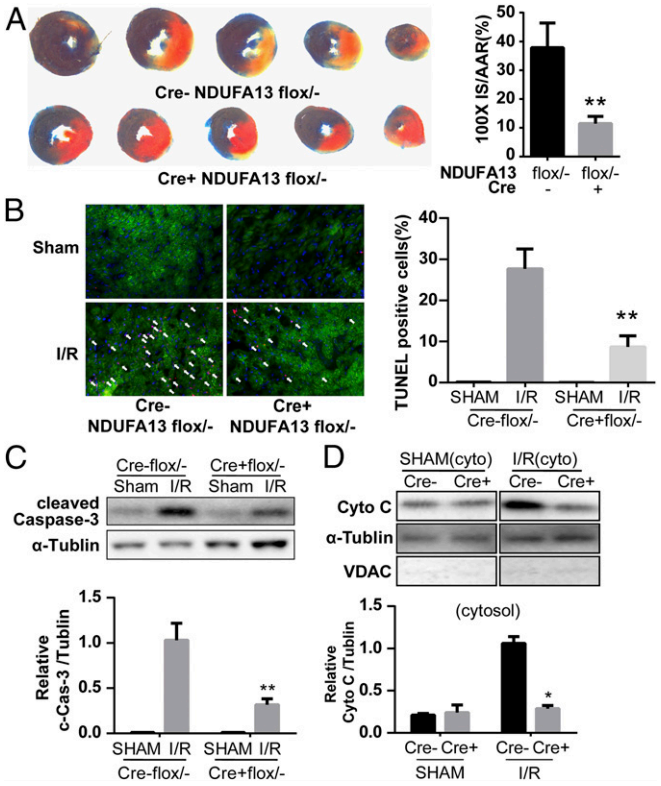

Fig. 3. (*A*) Both cHet (Cre+flox/-) and CON (Cre-flox/-) mice underwent either the I/R injury or the sham operation. IS was analyzed for both groups of mice with a representative 2,3,5-triphenyltetrazolium chloride (TTC) staining image and quantified in bar graph ($n = 5$ mice per group. $^{**}P < 0.01$ vs. Cre-flox/- mice). (*B*) TUNEL staining performed (white arrow indicates TUNEL-positive nucleus) and the quantification is shown in the bar graph ($^{**}P < 0.01$ vs. Cre-flox/- group). (*C*) Cleaved caspase-3 was also detected by Western blot with representative bands (α-tubulin was used as a loading control; $^{**}P < 0.01$ vs. Cre-flox/- I/R group, $n = 3$ mice per group). (*D*) Cytochrome *c* release was quantified by Western blot; VDAC, a mitochondrial marker was used as a quality control for the cytosol isolation, and α-tubulin used as a cytosol loading control ($n = 3$ mice per group. $^{*}P < 0.05$ vs. Cre-flox/- I/R mice).

STAT3 Is Responsible for the Cardioprotective Effects Caused by Moderate NDUFA13 Down-Regulation. To test the role of STAT3, NMCMs were isolated from the following mice: NDUFA13^{WT}STAT3^{WT} (wild-type), NDUFA13$^{flox/-}$STAT3^{WT} (NDUFA13 heterozygous), and NDUFA13$^{flox/-}$STAT3$^{flox/-}$ (double heterozygous) knock-down mice (for mice cross-breeding, see *SI Materials and Methods*) and then transfected with Ad-Cre. Native blue PAGE followed by Western blot analysis detected the formation of STAT3 dimers in NMCMs obtained from NDUFA13 heterozygous mice, which was absent when NMCMs were treated with *N*-acetyl-L-cysteine (NAC) or when STAT3 was simultaneously down-regulated (Fig. 5). The expression of peroxiredoxin 2 (PRX2), which can cause STAT3 dimerization (19), was increased in NMCMs from NDUFA13 heterozygous mice. The increased PRX2 expression can be attenuated by NAC, indicating the essential roles of ROS. In contrast, no changes in GPX expression levels were detected in these NMCMs (Fig. 5). STAT3 dimerization was responsible for up-regulated Bcl-2 expression as attenuation of STAT3 dimerization abolished the Bcl2 up-regulation (Fig. 5). Of note, the Ad-Cre–treated NMCMs isolated from STAT3$^{flox/-}$ mice exhibited a moderate decrease in STAT3 expression; however, it did not affect the dimerized level of STAT3 (Fig. S5) compared with Ad-Cre–treated NMCMs isolated from STAT3^{WT} mice (Fig. S5). The same were true with the levels of Bcl2 and PRX2 expression (Fig. S5).

Both cardiac-specific NDUFA13 heterozygous (Myh6Cre^{+}NDUFA13$^{flox/-}$STAT3^{WT}) and cardiac-specific double heterozygous (Myh6Cre^{+}NDUFA13$^{flox/-}$STAT3$^{flox/-}$) mice were treated with tamoxifen the same way as described above. Two weeks later, these mice were exposed to I/R injury. The cardiac protection against I/R injury offered by a moderate NDUFA13 was abolished when STAT3 was simultaneously down-regulated in mice as evidenced by an increase in IS (Fig. 6*A*), which also resulted in a reversal in TUNEL-positive cells in the peri-infarct area (Fig. 6*B*), as well as the cleaved caspase-3 expression (Fig. 6*C*). Of note, cardiac-specific STAT3 heterozygous knockout (Myh6Cre^{+}ER^{tam}STAT3$^{flox/-}$) and Myh6Cre^{+}ER^{tam}STAT3^{WT} mice that received tamoxifen treatment exhibited a similar degree of I/R injury as evidenced by IS (Fig. S6*A*), percentage of TUNEL staining-positive cells at peri-infarct area, and levels of cleaved caspase-3 (Fig. S6 *B* and *C*). Taken together, these data suggest that STAT3 is responsible for the cardioprotective effects against I/R injury when NDUFA13 expression is moderately down-regulated.

Discussion

In the present study, we generated a conditional cardiac-specific moderately down-regulated NDUFA13 mice, which were more tolerant to I/R injury, exhibited a smaller IS, and lower apoptotic activity. We then investigated ROS profile induced by mitochondria NDUFA13 down-regulation and detected a moderate increase in the levels of hydrogen peroxide, but not superoxide, in these mice. We have provided strong evidence to show that partial loss of NDUFA13 constitutes a structural substrate allowing for an electron leak such that a small amount of H_2O_2 would be continuously generated. As a result of a mild increase in hydrogen peroxide, up-regulated PRX2 expression occurred, leading to STAT3 dimerization and, hence, enhanced Bcl-2 expression, which were responsible for the protection offered by NDUFA13 down-regulation. Thus, we have not only elucidated a novel molecular mechanism of cardiac

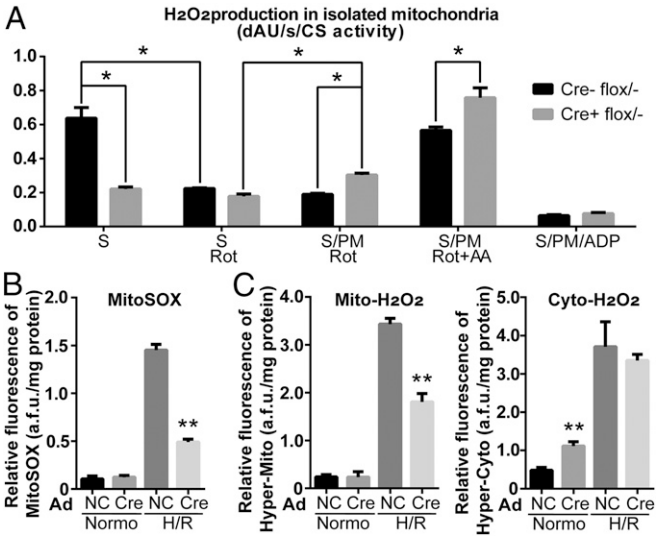

Fig. 4. (*A*) H_2O_2 measured in freshly isolated mitochondria from Cre+ ER^{tam}NDUFA13$^{flox/-}$ or Cre-ER^{tam}NDUFA13$^{flox/-}$ mice using Amplex Red as an indicator of fluorescence. Different substrates and blockers were used to differentiate the origin or mechanism of ROS generation induced by NDUFA13 down-regulation ($^{*}P < 0.05$). (*B*) NMCMs isolated from NDUFA13$^{flox/-}$ mice were treated with either Ad-NC or Ad-Cre and then used for quantification of superoxide generation at both the basal state and after an exposure to the H/R injury. The fluorescence intensity by mitoSOX red was measured by a microplate reader ($^{**}P < 0.01$, vs. Ad-NC–treated NMCMs exposed to H/R). (*C*) The same NMCMs used in *B* were infected with adenovirus containing either cyto-HyPer or mito-HyPer to measure H_2O_2 levels either at the basal state or after the H/R insult ($^{**}P < 0.01$, vs. Ad-NC–treated NMCMs at the same condition).

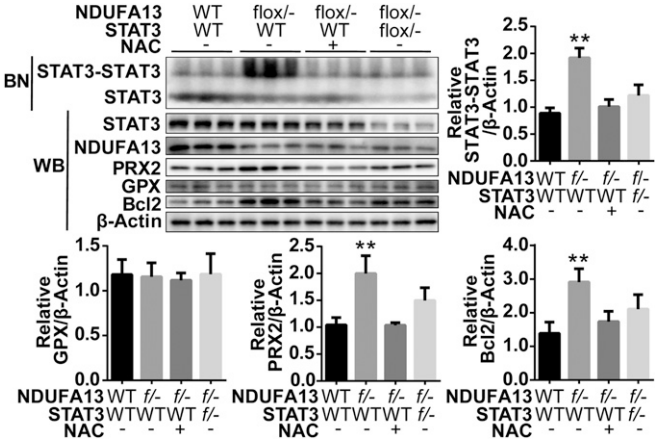

Fig. 5. NB-PAGE assay detected STAT3 oligomerization in heterozygous mice (Myh6Cre^{+}NDUFA13$^{flox/-}$STAT3^{WT}) that could be abolished by either NAC (ROS scavenger) or simultaneous STAT3 knockdown (Myh6Cre^{+}NDUFA13$^{flox/-}$STAT3$^{flox/-}$). NDUFA13, STAT3, GPX, PRX2, and Bcl2 expression levels were also quantified in each group of mice by Western blot, with β-actin as a loading control. $^{**}P < 0.01$ vs. Myh6Cre^{+}NDUFA13^{WT}STAT3^{WT} mice.

protection for which H_2O_2 functions as an important second messenger, more importantly we also have linked a unique profile of ROS to the specific molecule, NDUFA13, with its own molecular structure situated within the mitochondrial complex I.

Electron transfer across the different segments of mitochondrial complexes serves as a form of energy transduction, creating an electrochemical gradient across the inner membrane. It also dictates the form of ROS generated in both physiological and pathological states, such as the procession of I/R injury, due to the different electrochemical potentials pertaining to the different respiratory moieties (2, 3, 11). With normal oxygen supply, the short electronic effect of FMN is usually surpassed by the strong electron-withdrawing ability of its downstream FeS clusters (7). However, under oxygen deprivation conditions, the failure of electrons to react with their acceptor, oxygen, within complex IV sequentially saturates the FeS clusters and the FMN of complex I with electrons. Once the oxygen supply is restored, O_2 then can react with $FMNH_2$/FSQ, which is filled with electrons, to generate superoxides (in the form of $\bullet O_2^-$). This is a typical hypoxia-reperfusion scenario. $\bullet O_2^-$ is highly reactive, and the unpaired electrons on $\bullet O_2^-$ will capture any available electrons from molecules they may encounter, thus producing the relatively more stable H_2O_2. Although coenzyme Q is also filled with electrons, its reduction potential is +0.113 (7), which is insufficient for the production of $\bullet O_2^-$ ($O_2/\bullet O_2^-$ −0.13 V) but not H_2O_2 (O_2/H_2O_2 +0.70 V). H_2O_2 is a milder type of ROS than $\bullet O_2^-$. Under normal physiological conditions, a low level of H_2O_2 generation can mediate a variety of signaling events (20, 21).

Compared with prokaryotic cells, eukaryotic mitochondrial complex I has more nuclear-encoded subunits, which play essential roles in ensuring energy transduction along the mitochondria in a safe and efficient way (22). NDUFA13 is regarded as one of these accessory subunits and located at the heel position of mitochondrial complex I, with its helix segment inserted obliquely into hydrophobic chains ND1 and ND2 of complex I and TMH segment further anchored into the mitochondrial inner membrane (13). Using MOE software and the available database (PDB ID code: 5LDX), we did further analysis and noticed that the first 33 amino acids of NDUFA13 extend along the dorsal side of the CoQ binding chamber after penetrating the inner membrane and are parallel to the last three FeS clusters (N2, N6b, and N6a), which are ~31 Å apart. The enlarged tail of NDUFA13 remains on the intermembrane side of ND1 and ND2 (Fig. S7). The unique location and structure of NDUFA13 suggest that it may form a channel within complex I that interconnects the matrix with membrane interstitium (23). In the present study, we were mainly focused on elucidating the profile of ROS generated when NDUFA13 were down-regulated. Our data showed that moderate NDUFA13 knockdown resulted in an increase in H_2O_2 without involving in changes in MMP. We applied sequential experiments to test this notion that partial loss of NDUFA13 mainly resulted in an increase in H_2O_2. Data obtained from isolated mitochondria with Amplex red provided direct evidence of H_2O_2 generation secondary to NDUFA13 knockdown, which was confirmed by measuring superoxide within the mitochondria using mitoSOX red, showing no increase in superoxide generation at the basal state. Site-specific detection of H_2O_2 using cyto-HyPer and mito-HyPer further validated that H_2O_2 generated by partial loss of NDUFA13 was localized in the cytosol, but not in the mitochondria. Most importantly, a mild increase in H_2O_2 at the basal state can prevent the burst of superoxide generation following I/R injury. Taken together, we would propose our preliminary idea of a "spillhole theory" for which NDUFA13 serves as a guardian that gauges electron flow across the electron transfer chain, which should be closely related to the location and functional structure of NDUFA13 within mitochondrial respiratory complex I (Fig. S7).

Our present study also provided additional evidence that H_2O_2 promotes the formation of disulfide-linked STAT3 oligomers with the help of PRX2, which regulates the transcriptional activity of STAT3 to up-regulate Bcl2 expression (24), and renders tumor cells more

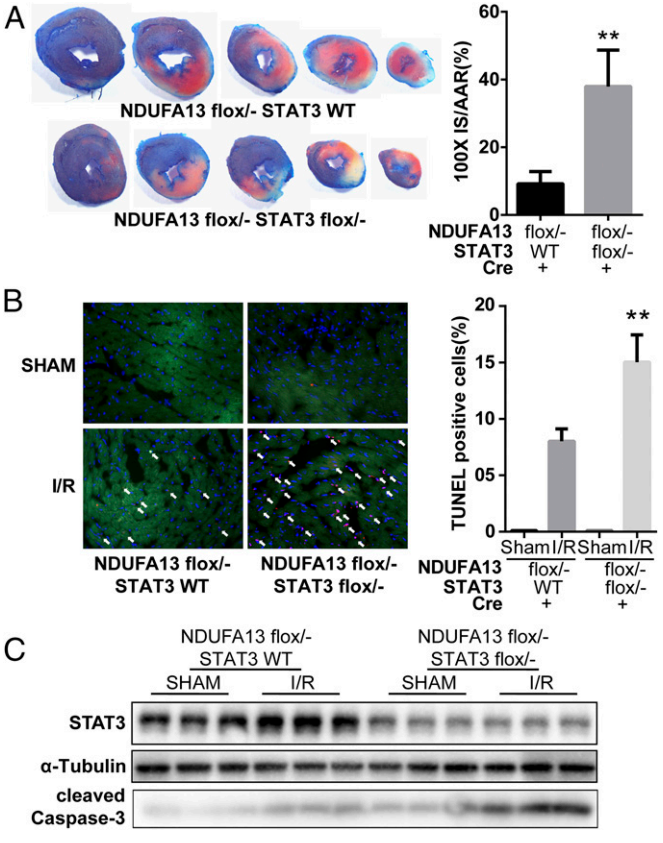

Fig. 6. (*A*) The NDUFA13 heterozygous (Myh6Cre^{+}NDUFA13$^{flox/-}$STAT3^{WT}) and NDUFA13 and STAT3 double heterozygous (Myh6Cre^{+}NDUFA13$^{flox/-}$STAT3$^{flox/-}$) mice were studied the same way as described in Fig. 3 and IS quantified ($^{**}P <$ 0.01 between the two groups). (*B*) TUNEL staining performed in the peri-infarct area and the percentage of TUNEL-positive cells (marked by white arrows) over total nuclei shown in the bar graph (n = 5 mice per group; $^{**}P < 0.01$ vs. NDUFA13 heterozygous I/R group). (*C*) STAT3 and cleaved caspase-3 expression levels measured by Western blot using the tissue of peri-infarct area from both group mice with α-tubulin as a loading control (n = 3 mice per group).

resistant to chemotherapy (15). The protection offered by down-regulated NDUFA13 through STAT3 signaling did not affect the extrinsic apoptotic pathway, as we did not observe significant changes in cleaved caspase-8 levels. In addition, the key components of the upstream molecule of intrinsic mitochondria-dependent apoptosis signaling pathway, such as ASK and JNK, were not affected. These changes indicate that the protection was mainly targeting the mitochondria.

In conclusion, a mild defective structure related to subunits of mitochondrial complex I, such as N2 with low electrochemical potential, can produce only H_2O_2, which can serve as a second messenger to activate STAT3/Bcl2, an important antiapoptotic signaling pathway. Thus, our study provided another protective mechanism against apoptosis induced by I/R injury.

Materials and Methods

Reagents. See *Supporting Information* for details.

Animals. Mice with a pair of loxP sites flanking exon3 of NDUFA13 (Fig. S8 and Table S2) were generated at the Shanghai Biomodel Organisms Center using standard methods and mated with FLP mice to excise the Neo cassette. MYH6-CreER^{tam} mice (25) (no. 005657) and STAT3$^{flox/flox}$ mice (no. 016923) from The Jackson Laboratory used for breeding various genotyping mice (see *Supporting Information* for detailed procedures). All procedures were approved by the Zhejiang University Institutional Animal Care and Use Committee and are in compliance with NIH Publication no. 85-23 (revised 1996). All mice were housed, bred, and maintained under specific pathogen-free (SPF) conditions.

Animal Model of I/R Injury. In brief, using a surgical approach, I/R injury was induced with 45 min of ischemia followed by 3 h of reperfusion. Sham surgical procedures were performed on the control group. IS was expressed as the percentage of the infarct area compared with the area at risk (for details, see *SI Materials and Methods*).

NMCMs with NDUFA13 Knockdown and Putback. NMCMs obtained from NDUFA13$^{flox/flox}$ mice were transfected with adenovirus containing Myh6-Cre to deplete endogenous NDUFA13, then infected with recombinant adenoviruses that expressed truncated mouse NDUFA13 cDNAs. The overexpression of various NDUFA13 mutants was confirmed by Western blot (for details, see *SI Materials and Methods*).

High-Resolution Respirometry. The Oxygraph-2k (O2k; OROBOROS Instruments) was used for measuring mitochondria respiration (26). Substrates and inhibitors were added sequentially to determine complex I, II, and IV respiration as indicated in the figure (for details, see *SI Materials and Methods*).

Detection of H_2O_2 and $\bullet O_2^-$ Production. H_2O_2 flux was measured simultaneously with respirometry in the O2k-Fluorometer using the H_2O_2-sensitive probe (10 μM Amplex UltraRed; Thermo Fisher A36006). For measurements of H_2O_2 production in intact cells, Ad-Cre or Ad-NC were infected with adenovirus carrying either Cyto-HyPer or Mito-Hyper (27). The intensity of fluorescence was measured by microplate reader. For superoxide measurements (28), the same designated NMCMs were studied and loaded with MitoSOX Red (5 mM for 10 min; Thermo Fisher M36008), and the intensity of fluorescence was measured by microplate reader (for details, see *SI Materials and Methods*).

For detailed information regarding Western blot, TUNEL staining, siRNA transfection mitochondria isolation, immunostaining, echocardiography, TEM, MMP determination, the quantification of H_2O_2 and $\bullet O_2^-$, native blue PAGE, H/R injury NMCM isolation (29), high-resolution respirometry, and NDUFA13 knockdown and putback, please refer to *SI Materials and Methods*.

Statistical Analysis. Data are presented as the mean ± SD. After confirming that all variables were normally distributed using the Kolmogorov–Smirnov test, unpaired Student's *t* test was used to determine the differences between two groups. $^*P < 0.05$ was considered as statistically significant.

ACKNOWLEDGMENTS. This work was supported by the National Basic Research Program of China (973 Program, Grants 2014CB965100 and 2014CB965103); National Natural Science Foundation of China [81320108003 and 31371498 (to J.W.), 81370346 (to W.Z.), 81622006 and 81670261 (to X.H.), and 81670235 (to Y.W.)]; Major Development Projects for Public Welfare, Grant 2013C37054 (to J.W.) and Major Scientific and Technological Projects, Grant 2013C03043-4 (to Y.S.) from Science and Technology Department of Zhejiang Province; and Grant Y201329862 (to W.Z.) from Education Department of Zhejiang Province.

1. Baradaran R, Berrisford JM, Minhas GS, Sazanov LA (2013) Crystal structure of the entire respiratory complex I. *Nature* 494:443–448.
2. Murphy MP (2009) How mitochondria produce reactive oxygen species. *Biochem J* 417:1–13.
3. Kussmaul L, Hirst J (2006) The mechanism of superoxide production by NADH:ubiquinone oxidoreductase (complex I) from bovine heart mitochondria. *Proc Natl Acad Sci USA* 103:7607–7612.
4. Liu Y, Fiskum G, Schubert D (2002) Generation of reactive oxygen species by the mitochondrial electron transport chain. *J Neurochem* 80:780–787.
5. Kushnareva Y, Murphy AN, Andreyev A (2002) Complex I-mediated reactive oxygen species generation: Modulation by cytochrome c and NAD(P)+ oxidation-reduction state. *Biochem J* 368:545–553.
6. Votyakova TV, Reynolds IJ (2001) DeltaPsi(m)-dependent and -independent production of reactive oxygen species by rat brain mitochondria. *J Neurochem* 79:266–277.
7. Sazanov LA (2007) Respiratory complex I: Mechanistic and structural insights provided by the crystal structure of the hydrophilic domain. *Biochemistry* 46:2275–2288.
8. Hirst J, King MS, Pryde KR (2008) The production of reactive oxygen species by complex I. *Biochem Soc Trans* 36:976–980.
9. Suzaki Y, et al. (2002) Hydrogen peroxide stimulates c-Src-mediated big mitogen-activated protein kinase 1 (BMK1) and the MEF2C signaling pathway in PC12 cells: Potential role in cell survival following oxidative insults. *J Biol Chem* 277:9614–9621.
10. Simon HU, Haj-Yehia A, Levi-Schaffer F (2000) Role of reactive oxygen species (ROS) in apoptosis induction. *Apoptosis* 5:415–418.
11. Chouchani ET, et al. (2014) Ischaemic accumulation of succinate controls reperfusion injury through mitochondrial ROS. *Nature* 515:431–435.
12. Nallar SC, Kalvakolanu DV (2017) GRIM-19: A master regulator of cytokine induced tumor suppression, metastasis and energy metabolism. *Cytokine Growth Factor Rev* 33:1–18.
13. Fearnley IM, et al. (2001) GRIM-19, a cell death regulatory gene product, is a subunit of bovine mitochondrial NADH:ubiquinone oxidoreductase (complex I). *J Biol Chem* 276:38345–38348.
14. Kalakonda S, et al. (2013) Monoallelic loss of tumor suppressor GRIM-19 promotes tumorigenesis in mice. *Proc Natl Acad Sci USA* 110:E4213–E4222.
15. Angell JE, Lindner DJ, Shapiro PS, Hofmann ER, Kalvakolanu DV (2000) Identification of GRIM-19, a novel cell death-regulatory gene induced by the interferon-beta and retinoic acid combination, using a genetic approach. *J Biol Chem* 275:33416–33426.
16. Zhang Y, et al. (2011) Downregulation of GRIM-19 promotes growth and migration of human glioma cells. *Cancer Sci* 102:1991–1999.
17. Nallar SC, et al. (2013) Tumor-derived mutations in the gene associated with retinoid interferon-induced mortality (GRIM-19) disrupt its anti-signal transducer and activator of transcription 3 (STAT3) activity and promote oncogenesis. *J Biol Chem* 288:7930–7941.
18. Alchanati I, et al. (2006) A proteomic analysis reveals the loss of expression of the cell death regulatory gene GRIM-19 in human renal cell carcinomas. *Oncogene* 25:7138–7147.
19. Sobotta MC, et al. (2015) Peroxiredoxin-2 and STAT3 form a redox relay for H2O2 signaling. *Nat Chem Biol* 11:64–70.
20. Peralta D, et al. (2015) A proton relay enhances H2O2 sensitivity of GAPDH to facilitate metabolic adaptation. *Nat Chem Biol* 11:156–163.
21. Winterbourn CC, Hampton MB (2015) Redox biology: Signaling via a peroxiredoxin sensor. *Nat Chem Biol* 11:5–6.
22. Guénebaut V, Schlitt A, Weiss H, Leonard K, Friedrich T (1998) Consistent structure between bacterial and mitochondrial NADH:ubiquinone oxidoreductase (complex I). *J Mol Biol* 276:105–112.
23. Vinothkumar KR, Zhu J, Hirst J (2014) Architecture of mammalian respiratory complex I. *Nature* 515:80–84.
24. Bhattacharya S, Ray RM, Johnson LR (2005) STAT3-mediated transcription of Bcl-2, Mcl-1 and c-IAP2 prevents apoptosis in polyamine-depleted cells. *Biochem J* 392:335–344.
25. Sohal DS, et al. (2001) Temporally regulated and tissue-specific gene manipulations in the adult and embryonic heart using a tamoxifen-inducible Cre protein. *Circ Res* 89:20–25.
26. Makrecka-Kuka M, Krumschnabel G, Gnaiger E (2015) High-resolution respirometry for simultaneous measurement of oxygen and hydrogen peroxide fluxes in permeabilized cells, tissue homogenate and isolated mitochondria. *Biomolecules* 5:1319–1338.
27. Karamanlidis G, et al. (2013) Mitochondrial complex I deficiency increases protein acetylation and accelerates heart failure. *Cell Metab* 18:239–250.
28. Robinson KM, et al. (2006) Selective fluorescent imaging of superoxide in vivo using ethidium-based probes. *Proc Natl Acad Sci USA* 103:15038–15043.
29. Zhang N, et al. (2016) Cardiac ankyrin repeat protein attenuates cardiomyocyte apoptosis by upregulation of Bcl-2 expression. *Biochim Biophys Acta* 1863:3040–3049.